RESEARCH ARTICLE

THE **FASEB** JOURNAL
The Journal of the Federation of American Societies for Experimental Biology

Novel immortalized human vocal fold epithelial cell line: In vitro tool for mucosal biology

Xia Chen[1] | Vlasta Lungova[1] ⬤ iD | Haiyan Zhang[2] | Chitrasen Mohanty[3] |
Christina Kendziorski[3] iD | Susan L. Thibeault[1]

[1]Division of Otolaryngology-Head and
Neck Surgery, Department of Surgery,
University of Wisconsin Madison, Madison,
WI, USA

[2]Department of Otolaryngology-Head and
Neck Surgery, Shandong Provincial ENT
Hospital, Cheeloo College of Medicine,
Shandong University, Jinan, P.R. China

[3]Department of Biostatistics & Medical
Informatics, University of Wisconsin
Madison, Madison, WI, USA

Correspondence
Susan L. Thibeault, Division of
Otolaryngology-Head and Neck Surgery,
Department of Surgery, University of
Wisconsin Madison, 5103 WIMR, 1111
Highland Ave, Madison, WI 53705-2275,
USA.
Email: thibeault@surgery.wisc.edu

Funding information
NIH - NIDCD, Grant/Award Number:
R01DC4336; NIH NIDCD, Grant/Award
Number: R01DC12773

Abstract
Study of vocal fold (VF) mucosal biology requires essential human vocal fold epithelial cell (hVFE) lines for use in appropriate model systems. We steadily transfected a retroviral construct containing human telomerase reverse transcriptase (hTERT) into primary normal hVFE to establish a continuously replicating hVFE cell line. Immortalized hVFE across passages have cobblestone morphology, express epithelial markers cytokeratin 4, 13 and 14, induced hTERT gene and protein expression, have similar RNAseq profiling, and can continuously grow for more than 8 months. DNA fingerprinting and karyotype analysis demonstrated that immortalized hVFE were consistent with the presence of a single cell line. Validation of the hVFE, in a three-dimensional in vitro VF mucosal construct revealed a multilayered epithelial structure with VF epithelial cell markers. Wound scratch assay revealed higher migration capability of the immortalized hVFE on the surface of collagen-fibronectin and collagen gel containing human vocal fold fibroblasts (hVFF). Collectively, our report demonstrates the first immortalized hVFE from true VFs providing a novel and invaluable tool for the study of epithelial cell-fibroblast interactions that dictate disease and health of this specialized tissue.

KEYWORDS
human vocal fold epithelial cells, immortalization, telomerase, three-dimensional VF mucosal model

1 | INTRODUCTION

Located in the larynx, and responsible for voicing, vocal folds (VF) are a pair of tissue shelves whose mucosa consists of two main cell types; VF stratified squamous epithelial cells cover and protect the lamina propria where VF fibroblasts produce extracellular matrix.[1] Interactions between these two cell populations dictate the architecture and biological function of VF mucosa which, in turn, determine ease of phonation, vocal quality, susceptibility to disease, and tissue repair outcomes. Because of the importance of epithelial cell-fibroblast interactions in shaping VF architecture and behavior in health, disease, and healing, as well as the significant costs associated with vocal dysfunction or disorders, it is imperative to

Abbreviations: 3D, three dimensional; EPC, epithelial cell culture; H&E, hematoxylin and eosin; HAS, human serum albumin; hTERT, human telomerase reverse transcriptase; hVFE, human vocal fold epithelial cell; hVFF, human vocal fold fibroblasts; IHC, immunohistochemical; VF, vocal fold.

understand how these two cell populations maintain VF homeostasis and coordinate mucosal tissue repair.

Epithelial cell-fibroblast interactions that define the biology of the VF mucosa, can be studied best in a controlled, in vitro environment. The development of human fibroblast cell (hVFF) lines by our group has made in vitro study of fibroblasts possible and important insights into the role of fibroblast behavior have been made as a result of having these robust cell lines. However, the difficulty of obtaining human vocal fold epithelial cells (hVFE) from primary sources, and the complete absence of hVFE lines, have severely limited the ability to advance the understanding of VF mucosa biology in disease processes, which are common among the general population. A lifetime prevalence of voice disorders has been reported at 29.9% for the adult population, with nearly 7% of adults report having current voice problems.[2]

VF epithelial cells are heterogenous in their phenotype, composed of basal and suprabasal cells with a limited proliferative capacity. The development of immortalized hVFE would extend the life span of these cells and provide an almost unlimited supply of cells for complex, continuous, long-term studies, and inter-laboratory comparisons of findings. There are several methods for immortalizing mammalian cells in culture. Viral genes, including Epstein-Barr virus (EBV), Simian virus 40 (SV40) T antigen, adenovirus E1A and E1B, and human papillomavirus (HPV) E6 and E7 can induce immortalization by a process known as viral transformation.[3] Although the process is reliable and relatively straight-forward, immortalized cells may become genetically unstable and lose the properties of primary cells. These viral genes typically achieve immortalization by inactivating the tumor suppressor genes that put cells into a replicative senescent state,[4] however, this also means that cell lines have the capacity to preferentially express tumor genes, which can alter the phenotype substantially. The preferred method for immortalizing cells is through expression of the human telomerase reverse transcriptase protein (hTERT). This gene is present but inactive in most somatic cells, when hTERT is exogenously expressed the cells are able to maintain telomeric lengths and thus avoid replicative senescence. Rigorous analyses of several telomerase-immortalized cell lines, including the immortalized hVFF cell lines created in our laboratory using this technique[5] have confirmed that the cells maintain a stable genotype and retain critical phenotypic markers in addition to normal karyotype.

The goal of the current work was to describe a method for in vitro primary culture and passaging of characterized hVFE from human VF tissue and to validate the proliferative hVFE cell line in an in vitro three-dimensional (3D) VF mucosa for the investigation of epithelial-fibroblast interactions. A 3D in vitro scratch wound model determined the applicability of the novel immortalized hVFE and highlighted how this model could be utilized to investigate important reciprocal interactions between immortalized hVFE and hVFF in tissue repair.

Taken together, immortalized hVFE and the 3D in vitro construct reported herein will have far reaching significance for future research in VF mucosal biology.

2 | MATERIALS AND METHODS

2.1 | Cells and culture

Primary normal hVFE (E67 and E80) were isolated from human true VF harvested from a 67-year-old female and 80-year-old male donors approximately 10-24 hours from death. The Institutional Review Board of the University of Wisconsin-Madison approved collection of tissue. For culture of hVFE from the tissue explant, cell culture plates were coated with rat tail collagen I 30 μg/mL, fibronectin 10 μg/mL, and BSA 10 μg/mL. After a 1-hour incubation to allow proteins to adsorb to the surface, the remaining solution was removed, and the surface was washed twice with PBS. The epithelial layer was carefully removed from the remainder of the tissue with sterile scissors and forceps; the epithelium was rinsed with 70% ethanol and PBS, cut into smaller pieces and placed on the pre-coated plates. Epithelial cell culture medium (EPC) was composed of airway epithelial basal medium (ATCC, Manassas, VA), human serum albumin (HAS) 500 mg/mL, linoleic acid 0.6 Mm, lecithin 0.6 mg/mL, L-glutamine 6 Mm, Extract P 0.4%, epinephrine 1.0 Mm, transferrin 5 mg/mL, T3 10 nM, hydrocortisone 5 mg/mL, rh EGF 5 ng/mL and rh insulin 5 mg/mL (ATCC), cholera toxin 25 μg/mL (Sigma, St. Louis, MO), and primocin 100 ng/mL (InvivoGen, San Diego, CA). After 10-14 days in primary culture, cells were passaged using low-concentration Trypsin-EDTA (0.05% Trypsin and 0.02% EDTA) for removing, contaminated fibroblasts. After 2-3 passages, hVFE (Figure 1) achieved 70%-90% confluence and were used for downstream assays.

Primary hVFF (T21) were isolated from the VF tissue from 21-year-old male donor and cultured in DMEM supplemented with 10% fetal bovine serum, 100 U/mL penicillin, 0.01 mg/mL streptomycin sulfate, and 1× NEAA (all from Sigma) as detailed in the previous study.[6] Passages 5-10 of primary hVFF were used for this study.

2.2 | Characterization of cultured cells

We characterized morphological features and cell markers of primary hVFE, primary hVFF, and immortalized hVFE by immunocytochemistry. Cells were cultured on coated slide chambers for 7-14 days and fixed for 15 minutes with 4% paraformaldehyde and blocked in 5% normal goat serum for 1 hour. Slides were incubated with primary antibodies at 4°C overnight and, after subsequent washes in PBS, species-specific fluorescence-conjugated secondary antibodies (Life Technologies Corporation, Carlsbad, CA) were applied
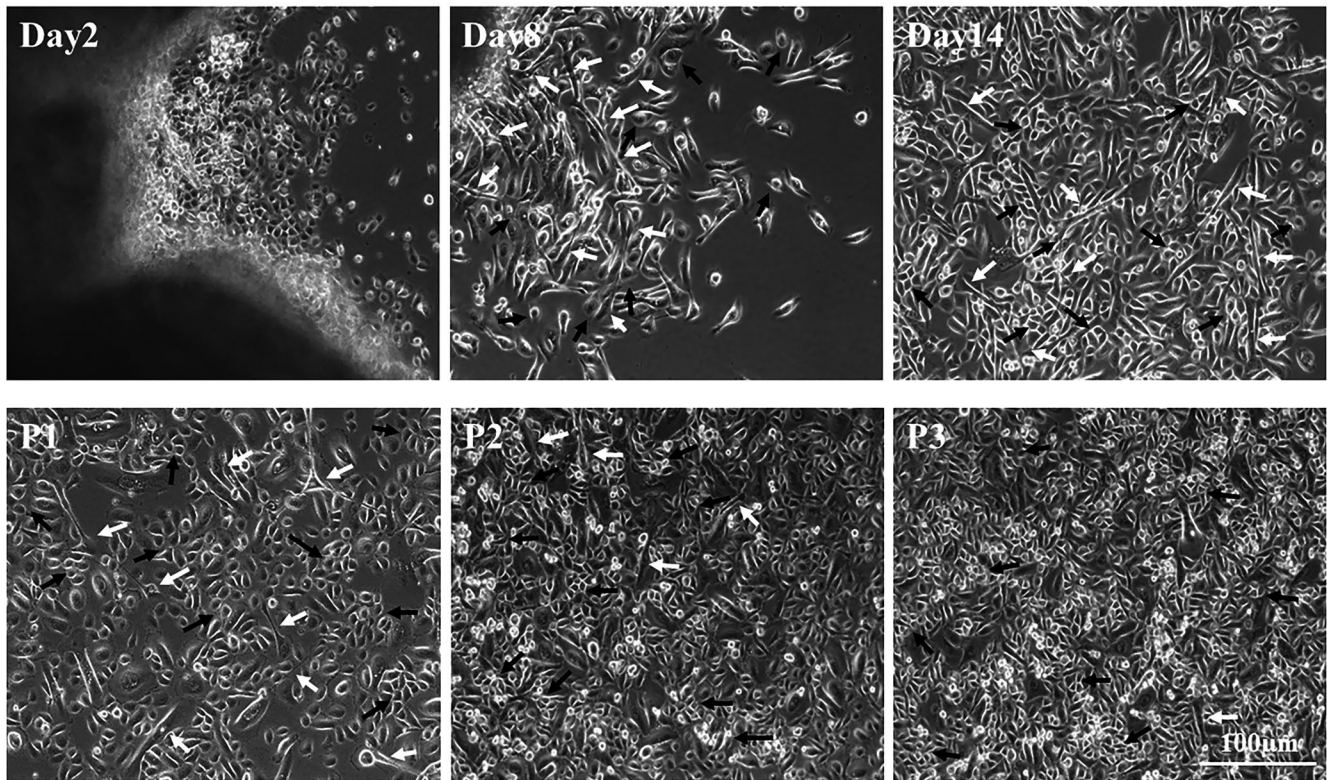
FIGURE 1 Morphology of primary hVFE from VF tissue samples, and their purification process under phase microscope. At Day 2, hVFE started growth from the edge of tissue, at Day 8 hVFF (white arrows) started mixed growth with hVFE (black arrows), at Day14 all hVFF and hVFE mixed growth together. After passing (P1, P2, and P3) with 0.05% trypsin, the mixed hVFF became less and less, hVFE population reached over 95% and demonstrated the typical "cobblestone" morphology. Scale bar: 100 μm

in the dark for 1 hour at room temperature (RT). DAPI dye provided nuclear staining. The following primary antibodies were used for immunocytochemistry: cytokeratin 4 (1:100, Abcam, Cambridge, MA), cytokeratin 13 (1:100, Abcam), cytokeratin 14 (1:50, Proteintech, Rosemont, IL), cytokeratin 18 (1:20, Abcam), collagen I (1:500, Abcam), fibronectin (1:200, Abcam), and hTERT (1:50, Abcam). Images were captured using a Nikon Eclipse E600 microscope (Nikon, Inc, Melvillin, NY) with Olympus DP71 digital camera (Tokyo, Japan).

2.3 | Retroviral vectors, transduction, and selection

Retroviral vector, pBABE-neo-hTERT (Addgene, Cambridge, MA), which contains SV40 promotor, hTERT gene, long terminal repeat (LTR) promotor sequence and a gene conferring neomycin resistance was utilized. Recombinant retroviruses were generated as previously described.[7] Briefly, plasmid DNA was transfected into a RetroPact PT67 packaging cell line (Clontech, Mountain View, CA). Following transfection, the total virus RNA of survival clones was isolated using a virus RNA isolation kit according to the manufacturer's protocol (Macherey-nagel GmbH & Co. KG, Düren, Germany) and viral titers were

assayed by quantitative polymerase chain reaction (qPCR) following the manufacture's procedures (Clontech). Clones with the highest titers (2.70×10^{14}–1.75×10^{15} copies/mL) were selected. Virus produced from the selected clones were used to infect human hVFE.

Active proliferating primary hVFE (passage 2 to 4) were seeded into 6-well plates at a density of 3×10^5 cells/well. When cells reached approximately 50%-60% confluence, medium was removed and 1.5 mL retroviral suspension with 4 μg/mL polybrene (MilliporeSigma, Burlington, MA), was added to the cells. Sixteen hours later, the viral supernatant was removed from the well and complete growth medium was added to the cells and incubated at 37°C. Re-infection was completed 24 hours later with the same procedure. Following infection and selection in G418 (100 μg/mL for 2 weeks), hVFE colonies were passed and expanded for further identification and investigation.

2.4 | Identification and characterization of immortalized hVFE

In order to identify and characterize that the hVFE were steadily transfected by a retroviral vector containing the hTERT gene, immortalized hVFE were analyzed by

polymerase chain reaction (PCR), telomerase activity assay, RNAseq, MTT proliferation assay, and immunocytochemistry. For PCR, total RNA extraction was performed using a RNeasy mini plus kit (Qiagen, Hilden, Germany). The quantity and quality of RNA were measured using a NanoDrop2000 Spectrophotometer (Thermo Scientific, Wilmington, DE). Human telomerase-specific primers (forward, 5′-GTGCTGGGCCTGGACGATATC-3″; reverse, 5′-GTAGCACAGGCTGCAGAGCAG-3″, product size 501 bp) were used. The PCR reaction were performed using a PCR machine with Go Taq Hot start polymerase (Promega, Madison, WI). The program consisted of initial denaturation 95ºC for 2 minutes, and 35 cycles of denaturation 95ºC for 30 seconds, annealing at 52ºC for 30 seconds, extension at 72ºC for 1min. PCR products were separated by 1.5% agarose gel electrophoresis and visualized with ethidium bromide, imaged by BioDoc-It imaging system (VUP, Upland, CA).

Telomerase activity was measured using PCR ELISA method, a PCR-based telomeric repeat amplification protocol (TRAP assay) which was performed using a Telo TAGGG Telomerase PCR ELISA Kit (Roche, Basel, Switzerland). This assay is based on specific amplification of telomerase-mediated elongation products combined with nonradioactive detection following an ELISA protocol. Briefly, 2×10^5 immortalized hVFE were isolated and lysed, and lysates were adjusted to 1×10^3 cells/µL. Negative controls were obtained by heat inactivation of telomerase at 85°C for 10 minutes. Telomeric repeat amplification was performed using 2 µL lysate. Elongation of primers by telomerase took place at 25°C for 20 minutes and telomerase was inactivated by 94°C for 5 minutes. Elongation products, as well as internal positive and negative controls included in the reaction vessel were amplified by PCR. PCR conditions were: 30 cycles of 94°C for 30 seconds, 50°C for 30 seconds, and 72°C for 90 seconds, followed by the elongation at 72°C for 10 minutes. PCR products were split into two aliquots, denatured and hybridized separately to digoxigenin-(DIG)-labeled detection probes, specific for telomeric repeats and for the internal standard. The resulting product was immobilized via the biotin-labeled primer to a streptavidin-coated microtiter plate. Immobilized PCR product was detected with anti-digoxigenin peroxidase using 3,3′, 5,5′-tetramethylbenzidine as a substrate. Color development was stopped after 15 minutes. Absorbance values of the samples were reported as $A_{450\ nm}$ reading against a blank (reference wavelength $A_{690\ nm}$) by FlexStation 3 absorbance plate reader (Bio-Tek instruments, Winooski, VT). Samples were regarded as telomerase-positive if the difference in absorbance ($\Delta A = A_{sample} - A_{negative}$) was higher than 0.2 $A_{450\ nm} - A_{690\ nm}$ units. These experiments were performed in triplicated and repeated twice.

To qualitatively assess the immortalized cells, using a previously published RNA-seq data set for primary hVFE cells comparisons were made between the newly immortalized VF cells at P1, P7, and P14. For RNA sequencing-Illumina assay, total RNA was extracted from immortalized hVFE (P1, P7, and P14) and primary hVFE using the RNeasy Mini Kit (Qiagen, Valencia, CA) according to the manufacture's instruction. RNA quantity and quality were assayed by Nanodrop1000, A260/280 is 1.8-2.1. RNA sequencing was performed by the University of Wisconsin-Madison Biotechnology Gene Expression Center and DNA Sequencing Facility. Quality control was done in FastQC v0.11.5 using standard defaults[8]; all samples passed and were used in downstream analysis.

To derive proliferation curves for primary and immortalized hVFE, cells were seeded in a 96-well culture plate at a density of 5000 cells/well and grown in EPC medium. After incubating for 24, 96, and 168 hours (h), cell proliferation rates were measured using a MTT cell proliferation assay (ATCC). On the day of measurement, 10µl MTT reagent was added into each well and incubated at 37ºC for 4h. When purple precipitate was visible under a microscope, 100 µL detergent reagent was add to each well, and left at RT in the dark for 4 hours to dissolve formazan crystals. MTT reduction was quantified by measuring light absorbance at 570 nm (reference wavelength 650 nm) using FlexStation 3 absorbance microplate reader (BioTek instruments). Each test was repeated at least four times.

2.5 | Genetic analysis

DNA fingerprinting and karyotype analysis were performed by Cell Line Genetics, Inc (Madison, WI). DNA was isolated from the immortalized hVFE cells using the DNA IQ system (Promega). One nanogram of DNA was amplified using the Powerplex 16 kit (Promega) and amplified DNA was run through an ABI 3730XL DNA analyzer. STR profiles were analyzed by Gene Marker HID (Softgenetics, State College, PA). Mitotically active cells in log phase were incubated with 130 ng/mL colcemid (Gibco, Ireland) treatment for 20-40 minutes at 37°C. Cells were dislodged with 0.05% Trypsin-EDTA into single cells and centrifuged at 1000 rpm. The cell pellet was resuspended in hypotonic 0.075 M KCl solution and fixed with methanol:glacial acetic acid (3:1) solution. Slides were prepared and baked at 90ºC for 1 hour before G-banding using trypsin-EDTA and Lieschman Stain (GTL). Slides were scanned and cells were imaged using the Leica GSL-120 slide scanner and cells were karyotyped using a CytoVysion digital imaging system.

2.6 | Creation of a human VF mucosal construct

Prior to seeding on constructs, immortalized hVFE (passages 10-20) were cultivated for in the DMEM stratified medium that was composed of DMEM/F12 medium with Glutamax (Gibco, Co Dublin, Ireland), supplemented with 10% B12 and 5% N2 (Gibco), 0.4 μg/mL hydrocortisone (Millipore Sigma) 8.4 ng/mL cholera toxin (Sigma), 5 μg/mL insulin (Millipore Sigma), 24 μg/mL adenine (Millipore Sigma), 20 ng/mL EGF, 100 U/mL penicillin, and 0.01 mg/mL streptomycin sulfate (Invitrogen, Carlsbad, CA). After 4 days, the cells were detached using 2 U/mL Dispase II (Millipore Sigma). Our 3D in vitro construct consisted of a collagen I gel seeded with primary hVFF, which served to mimic the collagen-rich VF lamina propria. Collagen-fibroblast constructs were prepared by combining high-concentration rat tail collagen I (final concentration of 4 mg/ml, 80% final volume; Corning, NY) and 10xDMEM (10% final volume; Sigma) on ice and adjusting pH with 1N NaOH. Primary hVFF T21, described previously[6] were resuspended in ice-cold fetal bovine serum (10% final volume; 5×10^5 cells/mL final volume) and added to the collagen mixture as described by others.[13-15] A mixture of collagen gel and hVFF was placed on transwell cell culture inserts (0.4 μm pore size, Corning), two milliliters per a 6-well culture insert, and solidified for 1 hour in a cell incubator at 5% CO2, 37ºC. Collagen was then gently detached with pasture pipette and constructs were flooded with DMEM stratified medium, returned into an incubator and left at least 24 hours to allow for gel contraction. The next day, immortalized hVFE were placed in clumps on collagen-fibroblast constructs at high density in 100 μL DMEM stratified medium. Cells were allowed to attach for at least 2 hours, then flooded with DMEM stratified medium and remained flooded for additional 4 days to allow proper attachment and expansion with medium changed every other day. Finally, the A/LI condition was initiated 4 days post seeding with flavinoid adenine dinucleotide (FAD) medium which consisted of the DMEM medium and F12 in ratio 1:3 (Gibco), supplemented with 2.5% FBS, 0.4 μg/mL hydrocortisone (Millipore Sigma), 8.4 ng/mL cholera toxin (Sigma), 5 μg/mL insulin, 24 μg/mL adenine (Millipore Sigma), 20 ng/mL epidermal growth factor, 100 U/mL penicillin, and 0.01 mg/mL streptomycin sulfate (Invitrogen) to initiate stratification. Medium was placed only in the basolateral chamber and changed three times a week. Cells were cultivated at A/Li interface for additional three weeks. Organotypic cultures of human VF mucosa were collected and characterized.

2.7 | Characterization of human VF mucosal construct

Human VF mucosal constructs were washed in PBS, fixed in fresh 4% paraformaldehyde for 15 minutes at RT, and embedded in HistoGel (Thermo Fisher Scientific). Constructs were dehydrated in series of ethanol, treated with xylene, embedded in paraffin, and cut to 5μm thick serial sections for hematoxylin and eosin (H&E) staining, and immunohistochemical (IHC) staining using standard protocols.[12] For IHC, sections were deparaffinized, rehydrated, and antigen retrieval was performed by heating sections in sodium citrate (pH 6) at 80°C water bath for 2 hours. After blocking in 5% goat serum for 90 minutes, sections were incubated with primary antibodies, anti-rabbit cytokeratin 4 (1:100, Abcam), anti-rabbit cytokeratin 13 (1:100, Abcam), anti-rabbit cytokeratin 14 (1:100, Proteintech), anti-rabbit E-cadherin (1:200, Cell Signaling, Danvers, MA), and anti-rabbit Laminin alfa 5 (1:100, Abcam) at 4°C overnight. Following with a secondary antibody, fluorescein anti-rabbit antibody (1:100 for 90 minutes at RT, Invitrogen), incubation, slides were mounted using Vectashield with DAPI (Vector Laboratories, Peterborough, UK), and images were captured with NikonE600 microscope (Nikon) and Olympus DP71 digital camera.

2.8 | In vitro scratch wound healing assay

One milliliter of solution containing collagen-fibronectin-BSA was pipetted into 12-well plate. After a 1-hour incubation to allow proteins to adsorb to the surface, the remaining solution was removed, and surface was washed twice with PBS. Immortalized hVFE were seeded on collagen-fibronectin-coated plate (as above described) and plate contained collagen gel with or without primary human hVFF T21 (as above described). A reference point was drawn on the bottom of each well. The plates were incubated until the cells reached confluence. Afterwards, epithelial cell monolayers were scratched with a sterile 200μl pipette tip to create cell-free area and washed with medium to remove any loose cells. Prior to imaging, the cultured cells were gently rinsed three times with medium. The cells at the same position along the scratch wound were imaged using an inverted phase-contrast microscope (Olympus CKX41) and Spot software (Version 5.2; Diagnostic Instruments) at day 0, 1, 3, 5, and 7. Images were further analyzed using ImageJ software to quantify the distance between migrated cells and wound edge. Day 0 was treated as our reference, wound width (pixel) was measured by ImageJ software for quantification of scratch wound assay. The progression of "healing" of the scratch wound, designed as migration in (%), was calculated in percent comparing scratch width at each time point to the initial scratch width at Day 0. Four independent experiments were completed.

2.9 | Statistical analysis

Telomerase activity (PCR ELISA), cell proliferation, and cell migration are expressed as mean $\pm$ standard deviations (SD)
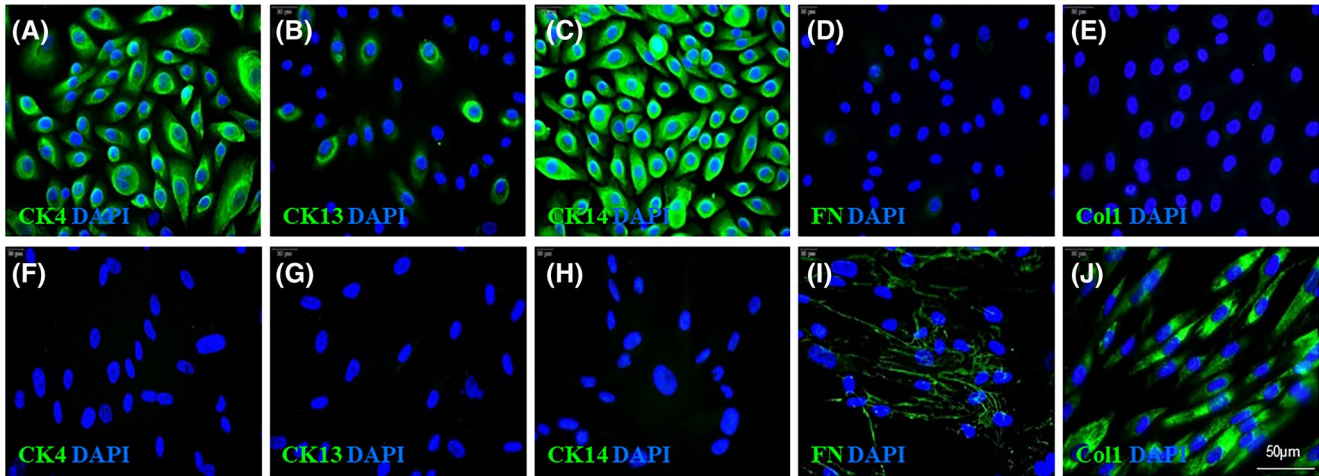
FIGURE 2   Identification of hVFE from hVFF. Immunocytochemistry revealed epithelial cell markers, cytokeratin 4 (CK4), cytokeratin 13 (CK13), and cytokeratin 14 (CK14), were positive in hVFE (A-C) and fibronectin (FN) and collagen I (Col1) were negative in hVFE (D and E). hVFF showed positive staining for FN (I) and Col1 (J), negative for CK4 (F), CK13 (G), and CK14 (H). Nuclei were counted-stained with DAPI. Scale bar: 50 µm
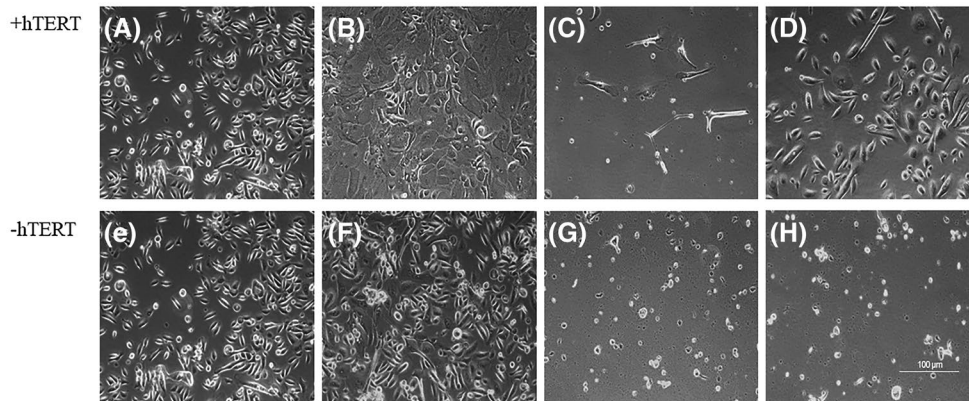

FIGURE 3   Process of hVFE immortalization. Primary hVFE (A) were transduced by retrovirus containing hTERT gene. Because large amounts of virus were applied, a significant number of cells underwent apoptosis (B). After 2-week G418 treatment (C), only a few cells survived with the transfection efficiency being less than 3%. After 5-week continued culture (D), cells that survived formed colonies. E-H shows control hVFE transfected by empty vector without hTERT gene. After 2-week G418 treatment (G) and 5-week additional culture (H), there were no living cells

of triplicated or quadruplicated samples per condition at each experiment, repeated three times. Telomerase activity, cell proliferation, and migration were assessed using a one-way ANOVA to compare telomerase activity OD readings, proliferation rates, and migration percentage at each time point with post hoc analyses. A p-value less than 0.05 was considered statistically significant. All analyses were performed using SAS statistical software version 9.1.3 (SAS Institute, Cary, NC).

For RNAseq analysis, reads were mapped back to the genome using the short-read aligner Bowtie v1.0.0,[13] followed by RSEM v1.2.7[14] to estimate gene expression. R/EBSeq[15] was applied to identify genes as differentially or equivalently expressed (DE or EE, respectively). EBSeq is an empirical Bayesian approach that models a number of features observed in RNA-seq data, and provides gene-specific posterior probabilities of DE and EE. A gene was labeled DE if the posterior probability of DE, PPDE, is greater than 0.95, which controls

the overall false discovery rate (FDR) at 5%; similarly, EE genes were those for which PPEE > 0.95. Enrichment of common functions was assessed using Enrichr[15,16] for GO biological processes analysis on each gene set. Enriched terms were sorted using score-based rankings to generate the top 10 enriched GO terms. For each comparison, two biological replicates and two technical replicates for primary cells and one biological replicate and one technical replicate for immortalized cells (n = 6) were used.

3 | RESULTS

3.1 | Isolation and cultivation of hVFE

The morphologic appearance of primary hVFE from tissue explant, and their purification process under phase microscope

are displayed in Figure 1. On day 2, hVFE cells grew from the edge of VF tissue sample, day 8 hVFF (white arrow) started their growth and mixed with hVFE (black arrow), day14 all hVFF and hVFE grew together until confluent. Because hVFE were very sensitive to Trypsin action, we selected 0.05% trypsin and shorter incubating time to detach hVFE from culture dishes. After three passages (P1, P2, and P3), the presence of hVFF were virtually eliminated; the final hVFE population reached approximately 95% pure and demonstrated typical "cobblestone" morphology.

3.2 | Characterization of hVFE

We utilized immunocytochemistry to characterize and confirm the etiology of primary cells were hVFE (Figure 2). First, we performed staining for typical markers of stratified squamous epithelium. hVFE expressed cytokeratin (CK) 4, which is a marker of the mucosal squamous epithelium (Figure 2A), CK13, a marker of suprabasal cells (Figure 2B) and CK14, a marker of the basal cellular compartment (Figure 2C). In parallel, we performed staining for typical fibroblast markers. hVFE were negative for fibronectin (Figure 2D) and collagen I (Figure 2E). Moreover, hVFF were negative for CK4, CK13, and CK14 (Figure 2F-H) and stained positive for fibronectin (Figure 2I) and collagen I (Figure 2J). These results demonstrate successful separation of hVFE and hVFF with hVFE maintaining VF epithelial cytokeratin markers.

3.3 | Immortalization and Identification of hVFE

Primary hVFE were transduced by the retrovirus containing hTERT gene (Figure 3A). Secondary to the large volume of virus applied, a substantial number of cells underwent apoptosis and death after a second transduction (Figure 3B). After 2 weeks of G418 selection, a few cells survived (Figure 3C) with a transfection efficiency of less than 3%. Following an additional 5 weeks of culture, the surviving cells maintained proliferation and formed colonies (Figure 3D). Figure 3E-H shows control hVFE transfected by empty vector without hTERT gene. After 2 weeks of G418 treatment (Figure 3G) and an additional 5 weeks of culture (Figure 3H), live cells could not be found.

Immortalized hVFE (T4) were confirmed and identified by standard PCR, PCR ELISA and immunocytochemistry (Figure 4). A standard PCR reaction showed a strong specific band of hTERT gene observed in the immortalized hVFE of passages 1, 7, 14, and 21 (Figure 4A). Telomerase activity of the immortalized hVFE was measured by PCR ELISA. Similarly, high level of telomerase activity was observed in the immortalized hVFE at passages 3, 7, 14, and 21 (2.880, 3.040, 3.031, and 3.018, respectively, $P = .071$, Figure 4B).
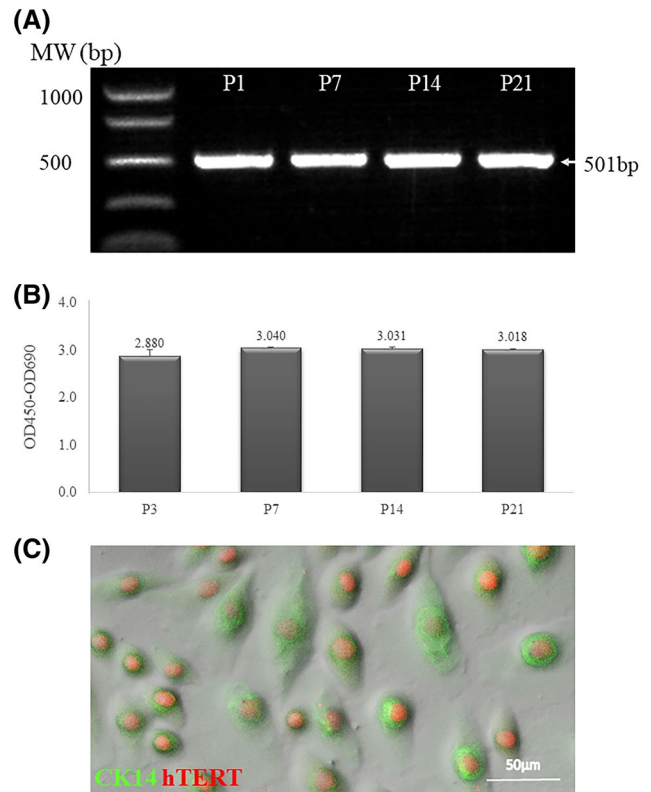
FIGURE 4 Immortalization of hVFE was identified and confirmed by standard PCR, PCR ELISA, and immunocytochemistry. A, PCR was performed following RNA extraction from immortalized hVFE at four different passages using the primers specific to hTERT gene and product was resolved on 1.5% agarose gel for confirming hTERT gene in immortalized hVFE. Strong hTERT gene expression (501bp band) was observed in immortalized hVFE at passages 1, 7, 14, and 21 (P1, P7, P14, and P21). B, telomerase activity of immortalized hVFE was measured by PCR ELISA. Similar level of telomerase activity was observed in immortalized hVFE at passages 3, 7, 14s and 21 (P3, P7, P14, and P21). C, cellular location of induced hTERT was identified by immunocytochemistry. Immortalized cells were labeled by epithelial cell marker, cytokeratin 14 (green), and hTERT (red) and imaged by confocal microscope demonstrating hTERT was positive in the nucleus of the epithelial cells. Scale bar: 50 μm

Confocal imaging (Figure 4C) showed induced hTERT accumulated in the nuclei (red) of the immortalized hVFE co-labeled with CK14 (green). These results confirmed that hTERT gene was successfully incorporated into the hVFE nucleus.

To assess whether immortalized hVFE cells were capable of maintaining their genotype during passaging and cell expansion, we conducted RNA-sequencing (RNA-seq) and compared transcriptional profiles of immortalized hVFE at passages P1, P7, and P14 to human adult primary hVFE characterized recently.[17] EBSeq analysis was applied to identify EE and DE genes with FDR controlled at 5% for each list. Our results show that from 16 966 sequenced genes in primary vs immortalized hVFE at P1, 8545 EE genes and 7329 DE were

found. Similar proportions of EE and DE genes were found in primary vs immortalized hVFE at P7 (8544 EE genes vs 7361 DE genes) and P14 (8724 EE genes vs 7057 DE genes). Across all conditions there were 6046 overlapping EE genes and 4940 DE genes. These results suggest that the immortalized cells share similarity to the primary cells and are stable in their expression across time.

Our data show that the top 10 EE enriched terms obtained from primary hVFE vs P1, P7, and P14 passages were mainly related to calcium ion transport (Tables 1 and 2), protein transport targeting the cell membrane and/or the endoplasmic reticulum (Tables 2 and 3) and cell signaling, such as positive regulation of cAMP-mediated signaling (Tables 2 and 3). Moreover, the top 10 DE enriched terms were involved in regulation of the mitotic cell cycle (Table 1), mitotic cell cycle transition from G2 to M phase (Tables 2 and 3), positive regulation of telomerase maintenance and lengthening (Table 3) as well as processes such as protein degradation associated with centromere assembly and nuclear envelope disassembly (Tables 1-3). When comparing the top 10 EE

and DE enriched terms across passages 3, 7, and 9 similar EE enriched terms and 2, 7, and 8 DE enriched terms were found. Taken together, these data show that immortalized hVFE are capable of maintaining their phenotype with almost comparable genotypes across cell passages. Moreover, similar to primary hVFE, immortalized hVFE are capable of carrying out their function related to ion and protein transport and cell signaling. DE genes, moreover, show that in contrast to primary hVFE, immortalized hVFE were successfully transformed and can generate the machinery important for successful mitotic cell division.

Under phase microscopy, immortalized hVFE (Figure 5A) showed similar cobblestone morphology as the primary hVFE (Figure 5B). However, hTERT expression (red) was present only in the immortalized hVFE (Figure 5C-E), not in primary hVFE (Figure 5F-H). Epithelial cell markers, cytokeratin CK 4, 13, and 14, were expressed in both immortalized hVFE (Figure 5I-K) and primary hVFE (Figure 5L-N) suggesting that immortalized hVFE maintained their epithelial phenotype. Next, we investigated short-term proliferation

TABLE 1 (a) GO biological processes analysis for top 10 equally expressed genes (EE) in primary hVFE and immortalized hVFE at passage P1. (b) GO biological processes analysis for top 10 differentially expressed genes (DE) in primary hVFE and immortalized hVFE at passage P1

Index	Name	*P*-value	Adjusted *P*-value	Odds ratio	Combined score
(a)					
1	negative regulation of interleukin-10 production (GO:0032693)	.0002905	.2118	2.16	17.59
2	membrane depolarization during action potential (GO:0086010)	.0001075	.1098	1.72	15.76
3	modulation of chemical synaptic transmission (GO:0050804)	.00005097	.1301	1.51	14.95
4	piRNA metabolic process (GO:0034587)	.0005081	.2881	1.95	14.79
5	positive regulation of NK T-cell activation (GO:0051135)	.002597	.4142	2.34	13.93
6	positive regulation of isomerase activity (GO:0010912)	.002597	.4016	2.34	13.93
7	terpenoid metabolic process (GO:0006721)	.002597	.4275	2.34	13.93
8	positive regulation of calcium ion-dependent exocytosis (GO:0045956)	.001235	.3318	2.01	13.43
9	cardiac myofibril assembly (DO:0055003)	.001001	.3193	1.93	13.31
10	membrane depolarization (GO:0051899)	.0003069	.1958	1.63	13.21
(b)					
1	regulation of cholesterol biosynthetic process (GO:0045540)	1.580e−7	.0001612	2.12	33.13
2	proteasome-mediated ubiquitin-dependent protein catabolic process (GO:0043161)	2.404e−10	.000001227	1.49	33.03
3	cellular protein modification process (GO:0006464)	1.242e−9	.000003168	1.25	25.55
4	microtubule anchoring at centrosome (GO:0034454)	.0001186	.01164	2.73	24.67
5	nuclear migration (GO:0007097)	.0001186	.01187	2.73	24.67
6	proteasomal protein catabolic process (GO:0010498)	6.779e−8	.0001153	1.46	24.14
7	regulation of mitotic cell cycle phase transition (GO:1901990)	3.188e−7	.002324	1.50	22.41
8	positive regulation of cell cycle arrest (GO:0071158)	.000002223	.001134	1.70	22.10
9	ubiquitin-dependent protein catabolic process (GO:0006511)	1.083e−7	.0001382	1.38	22.08
10	cytoplasmic sequestering of protein (GO:0051220)	.00009762	.01083	2.37	21.84

TABLE 2 (a) GO biological processes analysis for top 10 equally expressed genes (EE) in primary hVFE and immortalized hVFE at passage P7. (b) GO biological processes analysis for top 10 differentially expressed genes (DE) in primary hVFE and immortalized hVFE at passage P7

Index	Name	P-value	Adjusted P-value	Odds ratio	Combined score
(a)					
1	nuclear-transcribed mRNA catabolic process, nonsense-mediated decay (GO:0000184)	.000001306	.006664	1.53	20.67
2	SRP-dependent cotranslational protein targeting to membrane (GO:0006614)	.000002156	.003667	1.58	20.59
3	muscle contraction (GO:0006936)	.000001683	.004293	1.47	19.54
4	regulation of synapse assembly (GO:0051963)	.00003599	.02624	1.81	18.48
5	cotranslational protein targeting to membrane (GO:0006613)	.000007013	.008947	1.54	18.22
6	protein targeting to ER (GO:0045047)	.000008101	.008267	1.52	17.82
7	calcium ion transport (GO:0006816)	.000009160	.007791	1.47	17.03
8	positive regulation of cAMP-mediated signaling (GO:0043950)	.001107	.2825	2.34	15.93
9	regulation of lymphocyte proliferation (GO:0050670)	.0006021	.2363	2.03	15.04
10	piRNA metabolic process (GO:0034587)	.0005065	.2154	1.95	14.80
(b)					
1	DNA metabolic process (GO:0006259)	5.593e−17	2.854e−13	1.63	60.88
2	DNA replication (GO:0006260)	5.526e−13	1.410e−9	1.88	53.04
3	regulation of cholesterol biosynthetic process (GO:0045540)	2.826e−8	.00001803	2.17	37.78
4	DNA-dependent DNA replication (GO:0006261)	3.184e−8	.00001805	1.99	34.34
5	mitotic cell cycle phase transition (GO:0044772)	2.894e−10	4.923e−7	1.56	34.29
6	regulation of mitotic cell cycle phase transition (GO:1901990)	1.163e−9	.000001484	1.59	32.81
7	DNA biosynthetic process (GO:0071897)	3.771e−7	.0001132	2.09	30.91
8	centromere complex assembly (GO:0034508)	6.246e−7	.0001678	2.11	30.19
9	nuclear envelope disassembly (GO:0051081)	3.309e−7	.0001126	2.01	29.97
10	mitochondrial translational elongation (GO:0070125)	4.926e−8	.00002514	1.78	29.95

rates of immortalized and primary hVFE (Figure 5O). During a 7-day period, two primary cell lines at passage 2-3 showed rather flat proliferation curves, while immortalized hVFE at passage 3 presented a statistically significant raising growth, (P = .0009 and 0.0002, day 4 and day 7, respectively), as compared to primary cells. Immortalized hVFE maintained stable proliferative ability for more than 8 months, compared to primary hVFE, which stopped proliferating after three to four passages. These data show that hTERT gene was successfully incorporated into the genome, which significantly extended the lifetime of hVFE.

3.4 | Genetic analysis of immortalized hVFE

Next, we performed the karyotypic analysis. The DNA STR profile demonstrated that our immortalized epithelial cell line

was consistent with the presence of a single cell line, which did not match the DNA fingerprint pattern of any cell line published in ATCC, NIH, or DSMZ websites. Cytogenetic analysis was performed on 20 G-banded metaphase cells from the immortalized hVFE cell line, and all 20 cells demonstrated an abnormal female karyotype with trisomy 7, trisomy 20, loss of one copy of chromosome 11, and gain of two marker chromosomes of unknown origin (Figure 6).

3.5 | Identification of 3D human VF mucosal model

To address the potential of immortalized cells to differentiate into VF stratified squamous epithelium, we created 3D model of human VF mucosa (Figure 7A). Immortalized hVFE were seeded on the top of collagen-fibroblast

TABLE 3 (a) GO biological processes analysis for top 10 equally expressed genes (EE) in primary hVFE and immortalized hVFE at passage P14. (b) GO biological processes analysis for top 10 differentially expressed genes (DE) in primary hVFE and immortalized hVFE at passage P14

| Index	Name	*P*-value	Adjusted *P*-value	Odds ratio	Combined score
(a)					
1	muscle contraction (GO:0006936)	.000002055	.01049	1.46	19.06
2	omega-hydroxylase P450 pathway (GO:0097267)	.0005704	.1940	2.29	17.12
3	SRP-dependent cotranslational protein targeting to membrane (GO:0006614)	.00001300	.03317	1.52	17.10
4	protein targeting to ER (GO:0045047)	.00001806	.03072	1.49	16.26
5	positive regulation of cAMP-mediated signaling (GO:0043950)	.001308	.2903	2.29	15.22
6	nuclear-transcribed mRNA catabolic process, nonsense-mediated decay (GO:0000184)	.00004267	.05444	1.43	14.42
7	piRNA metabolic process (GO:0034587)	.0006641	.1993	1.91	13.98
8	modulation of chemical synaptic transmission (GO:0050804)	.00009898	.06314	1.48	13.66
9	cotranslational protein targeting to membrane (GO:0006613)	.00009031	.06583	1.45	13.54
10	positive regulation of NK T-cell activation (GO:0051135)	.003001	.4503	2.29	13.32
(b)					
1	DNA replication (GO:0006260)	6.222e−13	1.588e−9	1.91	53.77
2	DNA metabolic process (GO:0006259)	5.438e−15	2.775e−11	1.61	52.77
3	mitotic cell cycle phase transition (GO:0044772)	7.244e−11	1.232e−7	1.60	37.43
4	regulation of mitotic cell cycle phase transition (GO:1901990)	1.828e−10	2.332e−7	1.65	36.95
5	regulation of cholesterol biosynthetic process (GO:0045540)	5.867e−8	.00002722	2.20	36.57
6	positive regulation of telomere maintenance via telomere lengthening (GO:1904358)	1.755e−17	.00006396	2.25	35.01
7	DNA-dependent DNA replication (GO:0006261)	3.815e−8	.00001947	2.02	34.58
8	Mitochondrial translational elongation (GO:0070125)	0.034e−8	.00001720	1.82	31.58
9	DNA repair (GO:0006281)	7.347e−10	7.498e−7	1.50	31.46
10	mitochondrial translational termination (GO:0070126)	2.988e−8	.00001906	1.82	31.45

constructs, let differentiate at the A/Li for 3 weeks and then, collected for histological analyses. Our results show that after 3 weeks of culture of immortalized hVFE at the A/Li presented a typical multilayered stratified squamous phenotype (Figure 7B). Cells in the epithelium were positive for epithelial cell-specific markers, CK4 (Figure 7E) and 14 (Figure 7G). Cells in suprabasal layers showed positive staining for anti-CK13 (Figure 7F). The adherent junction marker, E-cadherin (Figure 7C) was also present in the constructed epithelium suggesting that the cells tightly adhered to each other and formed a compact epithelium. However, Laminin alfa 5 (Figure 7D), a component of the basement membrane was not observed in the construct.

These results indicate that immortalized hVFE are capable to differentiate into the multilayered epithelium that resembles the VF stratified squamous epithelium in its structure and function.

3.6 | Cell migration of hVFE

Finally, we investigated whether the immortalized hVFE cells could be utilized to create a 3D mucosa model with underlying VF fibroblasts to investigate wound healing and tissue repair. To test this, we created a scratch in a confluent layer of immortalized hVFE seeded on collagen gel without or with hVFF, and

FIGURE 5 Characterization of immortalized hVFE. Immortalized (A) and primary cultured hVFE (B) showed similar cobblestone morphology feature of epithelial cells; Immortalized cells were positively labeled by hTERT (red, D), comparing to primary hVFE (hTERT negative, G). DAPI (blue) was cell nuclei-counter stained (C, F), merged images of DAPI and hTERT in immortalized (E) and primary hVFE (H). Stratified epithelial cell markers, cytokeratin 4 (CK4), 13 (CK13), and 14 (CK14), were positively expressed in immortalized hVFE (I, J, K) and primary hVFE (L, M, N). DAPI (blue) was cell nuclei-counter stained. Scale bar: 50 μm; (O) Cell proliferation rates of immortalized and primary hVFE were measured by MTT assay. During 7-day period, two primary hVFE cells at passages 2-3 (◆ and ■) showed rather flat proliferation curves, while immortalized hVFE at passage 3 (▲) showed significant higher cell numbers at Day4 and Day7 compared with primary cells ($P = .0009$ and $P = .0002$, respectively)
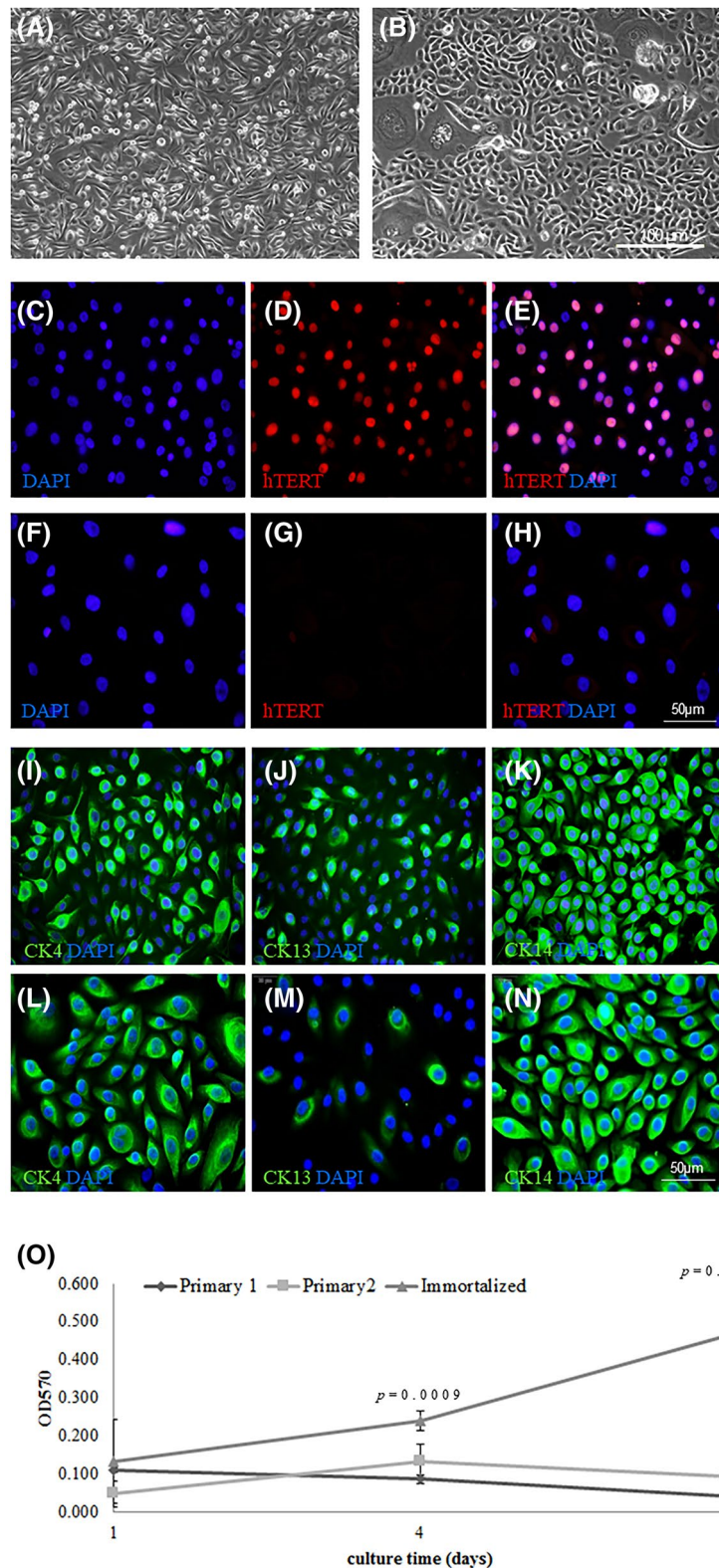
on collagen-fibronectin coated surface, and measured hVFE migration over 7 days in vitro. Visual analysis (Figure 8A) shows that hVFE starts to migrate into the wound within 24 hours on all these substrates. On a collagen gel without VFF migrated hVFE covered only about 20%-25% of the defect from day 3 to day 7 (Figure 8A). In collagen-fibroblast constructs there was a significantly higher rate of hVFE migration over a 7-day period compared to collagen gel alone ($P < .05$, Figure 8B). We found that on collagen-fibronectin surface hVFE migrated over half of the defect by day 3 and completely covered the defect by
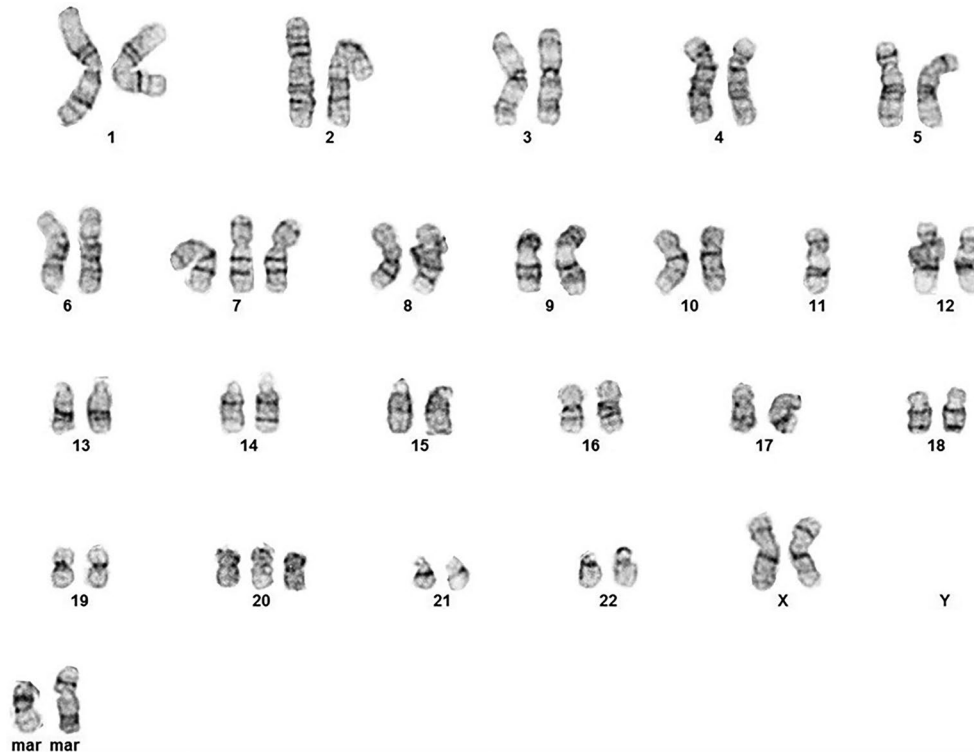
FIGURE 6 Cytogenetic analysis of immortalized hVFE cell line (passage 9) show an abnormal female karyotype with trisomy 7, trisomy 20, loss of one copy of chromosome 11, and gain of two marker chromosomes of unknown origin

day 5 in most trials; which was significantly faster than for the collagen gel constructs ($P < .05$, Figure 8B). Collectively we show that immortalized hVFE are capable of migration to initiate the wound closure and repair. The speed of immortalized hVFE migration likely depends on the presence of fibronectin and hVFF that enhance migration of epithelial cells.

4 | DISCUSSION

Primary culture of epithelial cells is challenging and difficult as these specialized cells depend upon cell to cell and cell to matrix interactions and require many growth factors, with loss of either leading to apoptosis and cell death. To date, limited primary culture of VF epithelial cells has been reported from porcine VF tissue and humans.[18,19] Immortalization of epithelial cells from various human tissues (subglottis, posterior commissure, and ventricles) that are in close proximity to and surround the true membranous VF have also been described.[20] In each of these aforementioned immortalizations, the type of human epithelial cells immortalized were pseudostratified ciliated epithelium which differs from the stratified squamous epithelium from the free edge of the true membranous VF. Herein we describe and characterize, to the best of our knowledge, the first generation of immortalized hVFE cells obtained from the luminal surface of the true VF.

Immortality of cell lines could be achieved by different approaches, including inactivating tumor suppressor genes (p53, Rb, and others) that can induce a replicative senescent state in cells[7,21] or introducing oncogenes.[22,23] We were successful in immortalizing our hVFE through the ectopic expression of TERT using pBABE-neo-hTERT retrovirus. Prior to our success with this methodology, we attempted Nucleofector technology,[24] which enables highly efficient transfection of primary cells, stem cells, neurons, and established cell lines as well as other nonviral transfection methods, such as a Cytofect Epithelial Cell Transfection Kit,[25] which is a plasmid DNA delivery system designed especially for epithelial cells. Unfortunately, none of these methods were successful suggesting that retroviral transfection is currently a method for efficient TERT gene nuclear delivery.

The TERT gene is inactive in most somatic cells, but when it is exogenously expressed cells are able to maintain sufficient telomere lengths to avoid replicative senescence. However, overexpression of hTERT in some cell types can be challenging, especially in primary epithelial cells. To overcome these problems, we applied a very high-titer recombinant retrovirus (approximately1000-times concentrated virus used for normal transfection-2.4×10^{11}copies/mL)[26] to our primary hVFE cell cultures, which also resulted in a very low transfection efficiency, and generated one positive cell clone (out of more than 20 plated) that maintained proliferation for more than 8 months and beyond, without presenting signs
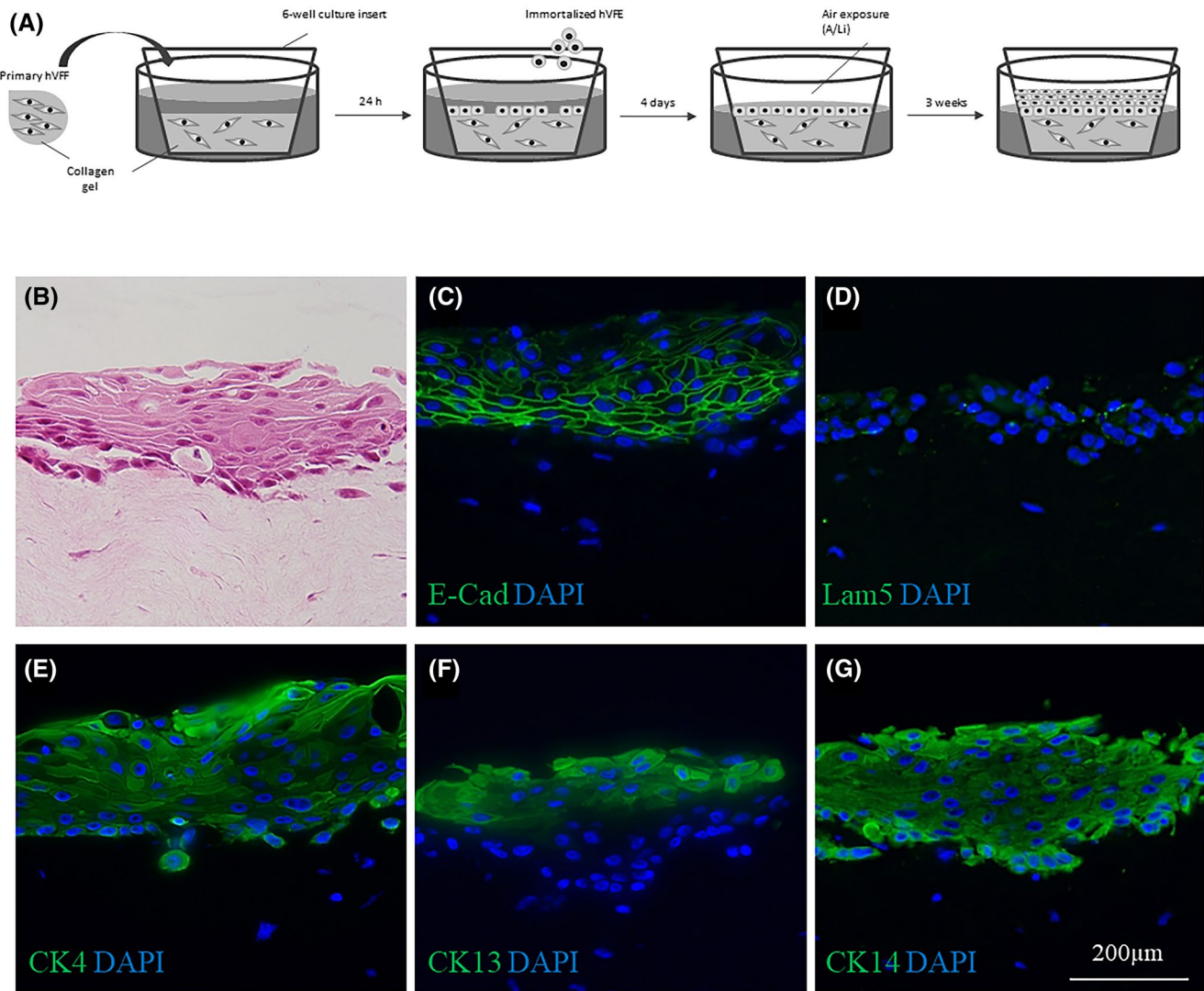
FIGURE 7 Characterization of immortalized hVFE in 3D VF mucosa construct. A, Schematic of VF mucosa construct by co-culturing of immortalized hVFE and primary hVFF. B, H&E staining shows morphology of the VF mucosa construct developed with immortalized hVFE. C, Anti-E-cadherin staining shows E-cadherin expressed in all layers of immortalized hVFE. D, Anti-Laminin alfa 5 staining demonstrates lack of basement membrane found in developed VF mucosa construct. E-G, IHC staining for stratified epithelial markers, CK4 (E), CK13 (F), and CK14 (G). CK4 and CK14 were expressed in all layers of hVFE, CK13 expressed in super-basal layers of epithelium. DAPI (blue) was cell nuclei-count stain. Scale bar: 200 μm

of senescence. In earlier reports, multiple human epithelial subsites have been immortalized by SV40 or HPV E6/E7, including ovarian, subglottic, esophageal, and corneal.[3,20,27,28] Furthermore, previous work report that human epithelial cells from airway, nasopharyngeal, and ovarian were immortalized with combination of oncogene expression and activation of telomerase.[4,29,30] Use of both virus oncogenes, such as HPV E6/7 and SV40 T antigen and expression of hTERT has produced immortal epithelial cell lines with abrogated cell cycle control and apoptosis machinery, with spontaneous malignant transformation during prolong culture.[31,32] In our approach, we avoided using viral oncoproteins as these proteins inactive both Rb and p53 pathways.[4] We demonstrated that hTERT alone was sufficient for cell immortalization,

similar to a previous report,[33] albeit with small variations in their karyotype, similar to other reports in epithelial cells immortalized via hTERT[33-37] Investigators have suggested that small variations in chromosomes may contribute to cellular immortalization.[35,36] However, chromosomal gain could also be the result of mitotic nondisjunction due to integration of the proviral cDNA into the cell's genome after retroviral transfection.[35] Ramirez et al have reported comparable studies for immortalized human bronchial epithelial cells lines and parental cells.[35] Their results showed that despite duplication of parts of chromosomes 5 and 20 in their immortalized cell lines, the cells had intact p53 checkpoint pathways, which impact cellular homeostatic mechanisms that monitor DNA replication, chromosome segregation and cell division.[38]
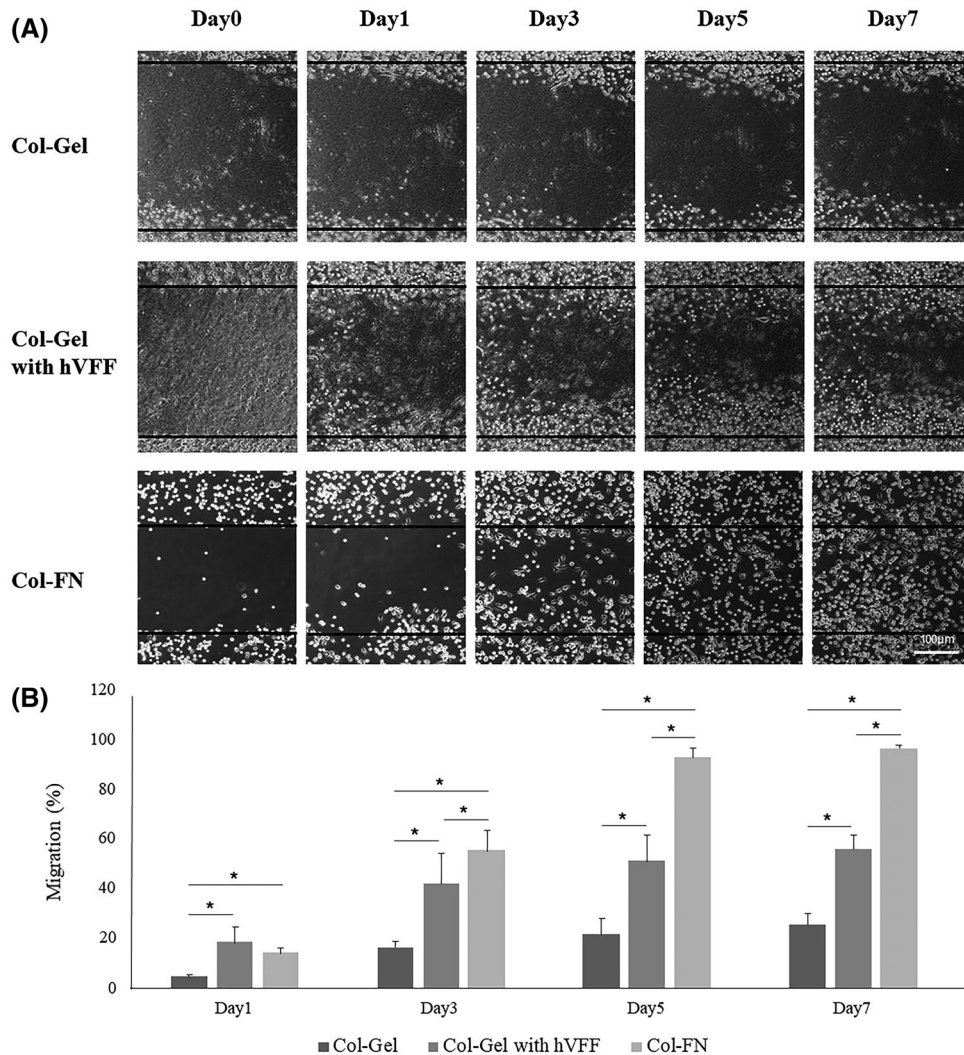
FIGURE 8 Cell migration evaluation of immortalized hVFE from the surface of collagen gel, collagen gel with primary hVFF, and collagen-fibronectin coated plate. A, Immortalized hVFE were grown on the surface of the collage gel (4 mg/mL collagen I, Col-Gel), collagen gel containing hVFF (Col-Gel with hVFF), and collagen-fibronectin coated plate (30 µg/mL collagen I and 10 µg/mL fibronectin, Col-FN) until confluent. A cell-free area was introduced with a pipette tip, and migration was evaluated after 24 hours. Representative examples of cells at Day 0, 1, 3, 5, and 7 from four independent experiments are shown. Scale bar: 100 µm. B, Quantification of the results of four separated scratch wound assays using ImageJ. On Col-FN surface, cells began to infiltrate the wound area by Day 1 and completely covered the wound by Day 5, compared to cells on Col-Gel that had 20%-30% of the area covered over the same 7-day period. On collagen gel with fibroblasts, by Day 3 epithelial cell migration covered the 40% of the wound and by Day 5-7 covered 60% of the wound. Asterisks (*) indicate a significant difference ($P < .05$) in scratch wound healing compared to the different substrate at same time point

Further investigation of the effect of the chromosomal alternations found in our cells warrant investigation, however our RNAseq results indicate similar cell functions and signaling.

To validate the differentiation potential of immortalized hVFE, we created a 3D model of human VF mucosa using immortalized hVFE and primary hVFF and assessed the expression of key stratified markers which were similar to native human VF mucosa.[9,39] Our immortalized hVFE showed similar cell morphologic features and cell markers as the primary hVFF, similar with our previous work with iPSC-derived VFE in a VF mucosa model.[17] The difference is that iPSC-derived VFE can be induced from iPSC over the course of a month, but the immortalized hVFE can be easily

frozen, stored, and recovered. It can be shipped to other research institutions and widely used for various in vitro research in laryngeal field. Specialized training and time for culture is mitigated Unfortunately, Laminin-alfa 5, a basal membrane component, was not expressed in our model suggesting that anchorage of immortalized hVFE to collagen matrix could be impaired and/or immature. These results are similar to work utilizing primary hVFE in a 3D VF mucosa construct.[19] In this investigation the developed 3D model of human VF provides a valuable tool for investigation of human VF in physiological and pathological conditions.

Wound healing is a complex process which involve extracellular matrix (ECM) components, multiple kinds of

cells (epithelial cells, fibroblasts, and macrophages), and various secreted growth factors.[40] In previous reports, fibroblasts play a key role in the deposition and remodeling of ECM components and wound.[41] Epithelial cell migration during the wound healing process is an important step to complete healing when the VF are injured.[42] The vast majority of existing wound healing models use only one type of ECM protein and one cell type whereby lacking the complexity of the wound bed microenvironment.[43,44] In this study, we present a novel 3D wound healing model that closely mimics the VF environment allowing study of hVFE cell migration and regulation between hVFE and hVFF. We plated of our immortalized hVFE on 3D collagen-fibroblast construct and controls being collagen gel alone and collagen-fibronectin coated plates. We found that the migration of immortalized hVFE on collagen-fibroblast constructs was significantly faster than in the model without fibroblasts. These results suggest that fibroblasts promote migration of epithelial cells, which might be caused by the growth factors released from fibroblasts and ECM components (such as fibronectin and collagen).[45] This is in agreement with previous study demonstrating that exogenous epidermal growth factor can increase the rate of wound healing in an embryonic stem cell-derived model of VF mucosa.[46] Notably, the fastest migration occurred when the immortalized hVFE were cultured on culture dishes coated with collagen-fibronectin. These findings indicate that fibronectin can also enhance the migration of VF epithelial cells as reported previously for fibroblasts[47] or vascular smooth muscle cells.[48] However, our culture system cannot distinguish between the role of fibronectin and the stiffness of the substrate, which can facilitate migration as well. Further experiments utilizing this novel construct are needed to provide the evidence about the role of fibronectin and various growth factors in stimulation of VFE migration during wound closure and elucidate the possible mechanisms involved in the VF wound healing.

In summary, this report provides the scaffold for the proficient generation of immortalized hVFE from primary culture with validation of their usefulness in a 3D in vitro VF mucosa model. This tool will allow for the improved understanding of the reciprocal interactions between epithelial cells and fibroblasts in VF mucosal biology whereby providing an opportunity for disease modeling and testing therapeutic approaches for the treatment of VF remodeling, inflammation, or other laryngeal diseases.

CONFLICT OF INTEREST
The authors have stated explicitly that there are no conflict of interest in connection with this article.

AUTHOR CONTRIBUTIONS
X. Chen and S. Thibeault designed research; X. Chen, V. Lungova, and H. Zhang performed research; X. Chen and V. Lungova analyzed data; X. Chen, V. Lungova, and S. Thibeault wrote paper; C. Mohanty and C. Kendziorski analyzed RNA data.

ORCID
Vlasta Lungova https://orcid.org/0000-0002-5723-3441
Christina Kendziorski https://orcid.org/0000-0002-0700-6267

REFERENCES
1. Hirano M. Morphological structure of the vocal cord as a vibrator and its variations. *Folia Phoniatr*. 1974;26:89-94.
2. Roy N, Merrill RM, Gray SD, Smith EM. Voice disorders in the general population: prevalence, risk factors, and occupational impact. *Laryngoscope*. 2005;115:1988-1995.
3. Shin HY, Yang W, Lee EJ, et al. Establishment of five immortalized human ovarian surface epithelial cell lines via SV40 T antigen or HPV E6/E7 expression. *PLoS ONE*. 2018;13:e0205297.
4. Smith JL, Lee LC, Read A, et al. One-step immortalization of primary human airway epithelial cells capable of oncogenic transformation. *Cell Biosci*. 2016;6:57.
5. Chen X, Thibeault SL. Novel isolation and biochemical characterization of immortalized fibroblasts for tissue engineering vocal fold lamina propria. *Tissue Eng. Part C*. 2009;15:201-212.
6. Chen X, Thibeault SL. Characteristics of age-related changes in cultured human vocal fold fibroblasts. *Laryngoscope*. 2008;118:1700-1704.
7. Lundberg AS, Hahn WC, Gupta P, Weinberg RA. Genes involved in senescence and immortalization. *Curr Opin Cell Biol*. 2000;12:705-709.
8. Andrews S. FastQC: a quality control tool for high throughput sequence data. 2010. http://www.bioinformatics.babraham.ac.uk/projects/fastqc
9. Leydon C, Selekman JA, Palecek S, Thibeault SL. Human embryonic stem cell-derived epithelial cells in a novel in vitro model of vocal mucosa. *Tissue Eng Part A*. 2013;19:2233-2241.
10. Metallo CM, Ji L, de Pablo JJ, Palecek SP. Retinoic acid and bone morphogenetic protein signaling synergize to efficiently direct epithelial differentiation of human embryonic stem cells. *Stem Cells*. 2008;26:372-380.
11. Lungova V, Leydon C, Thibeault SL. Derivation of epithelial cells from human embryonic stem cells as an in vitro model of vocal mucosa. *Methods Mol Biol*. 2016;1307:237-243.
12. Lungova V, Verheyden J, Herriges J, Sun X, Thibeault SL. Ontogeny of the mouse vocal fold epithelium. *Dev Biol*. 2015;399:263-282.
13. Langmead B, Trapnell C, Pop M, Salzberg SL. Ultrafast and memory-efficient alignment of short DNA sequences to the human genome. *Genome Biol*. 2009;10:R25.

14. Li B, Dewey CN. Rsem: accurate transcript quantification from RNA-seq data with or without a reference genome. *BMC Bioinforma*. 2011;12:323.

15. Leng N, Dawson JA, Thomson JA, et al. EBSeq: an empirical Bayes hierarchical model for inference in RNA-seq experiments. *Bioinformatics*. 2013;29:1035-1043.

16. Chen EY, Tan CM, Kou Y, et al. Enrichr: interactive and collaborative HTML5 gene list enrichment analysis tool. *BMC Bioinforma*. 2013;14:128.

17. Lungova V, Chen X, Wnag Z, Kendziorski C, Thibeault SL. Human induced pluripotent stem cell-derived vocal fold mucosa mimics development and responses to smoke exposure. *Nat Commun*. 2019;10:4161.

18. Erickson-DiRenzo E, Leydon C, Thibeault SL. Methodology for the establishment of primary porcine vocal fold epithelial cell cultures. *Laryngoscope*. 2019;129:E355-E364.

19. Ling C, Li Q, Brown ME, et al. Bioengineered vocal fold mucosa for voice restoration. *Sci Transl Med*. 2015;18(7):314.

20. Powell J, Verdon B, Wilson JA, Simpson AJ, Pearson J, Ward C. Establishment of an immortalized human subglottic epithelial cell line. *Laryngoscope*. 2019;129:2640-2645.

21. Shay JW, Wright WE, Werbin H. Defining the molecular mechanisms of human cell immortalization. *Biochim Biophys Acta*. 1991;1072:1-7.

22. Tsao SW, Wang X, Liu Y, et al. Establishment of two immortalized nasopharyngeal epithelial cell lines using SV40 large T and HPV16E6/E7 viral oncogenes. *Biochim Biophys Acta*. 2002;1590:150-158.

23. Halbert CL, Demers GW, Galloway DA. The E7 gene of human papillomavirus type 16 is sufficient for immortalization of human epithelial cells. *J Virol*. 1991;65:473-478.

24. Iversen N, Birkenes B, Torsdalen K, Djurovic S. Electroporation by nucleofector is the best nonviral transfection technique in human endothelial and smooth muscle cells. *Genet. Vaccines Ther*. 2005;3:2.

25. Alvarez J, Gagnon D, Coutlée F, Archambault J. Characterization of an HPV33 natural variant with enhanced transcriptional activity suggests a role for C/EBPβ in the regulation of the viral early promoter. *Sci. Rep*. 2019;9:5113.

26. Hu P, Li Y, Sands MS, McCown T, Kafri T. Generation of a stable packaging cell line producing high-titer PPT-deleted integration-deficient lentiviral vectors. *Mol Ther Methods Clin Dev*. 2015;2:15025.

27. Inokuchi S, Handa H, Imai T, et al. Immortalisation of human oesophageal epithelial cells by a recombinant SV40 adenovirus vector. *Br J Cancer*. 1995;71:819-825.

28. Kim CW, Park GT, Bae ON, Noh M, Choi KC. Application of SV40 Transformed human corneal epithelial cells to evaluate potential irritant chemicals for in vitro alternative eye toxicity. *J Pharmacol Toxicol Methods*. 2016;80:82-89.

29. Yip YL, Pang PS, Deng W, et al. Efficient immortalization of primary nasopharyngeal epithelial cells for EBV infection study. *PLoS ONE*. 2013;8:e78395.

30. Yang G, Rosen DG, Mercado-Uribe I, et al. Knockdown of p53 combined with expression of the catalytic subunit of telomerase is sufficient to immortalize primary human ovarian surface epithelial cells. *Carcinogenesis*. 2007;28:174-182.

31. Hurlin PJ, Kaur P, Smith PP, Perez-Reyes N, Blanton RA, McDougall JK. Progression of human papillomavirus type 18-immortalized human keratinocytes to a malignant phenotype. *Proc Natl Acad Sci*. 1991;88:570-574.

32. Gregorie L, Rabah R, Schmelz EM, Munkarah A, Roberts PC, Lancaster W. Spontaneous malignant transformation of human ovarian surface epithelial cells in vitro. *Clin Cancer Res*. 2001;7:4280-4287.

33. Li NF, Broad S, Lu YJ, et al. Human ovarian surface epithelial cells immortalized with hTERT maintain functional pRb and p53 expression. *Cell Prolif*. 2007;40:780-794.

34. Garbe JC, Vrba L, Sputova K, et al. Immortalization of normal human mammary epithelial cells in two steps by direct targeting of senescence barriers does not require gross genomic alterations. *Cell Cycle*. 2014;13:3423-3435.

35. Ramirez RD, Sheridan S, Girard L, et al. Immortalization of human bronchial epithelial cells in the absence of viral oncoproteins. *Cancer Res*. 2004;64:9027-9034.

36. Gu Y, Li H, Miki J, et al. Phenotypic characterization of telomerase-immortalized primary non-malignant and malignant tumor-derived human prostate epithelial cell lines. *Exp Cell Res*. 2006;312:831-843.

37. Troester MA, Hoadley KA, Sorlie T, et al. Cell-type-specific responses to chemotherapeutics in breast cancer. *Cancer Res*. 2004;64:4218-4226.

38. Vogelstein B, David Lane D, Levine AJ. Surfing the p53 network. *Nature*. 2000;408:307-310.

39. Leydon C, Imaizumi M, Bartlett RS, Wang SF, Thibeault SL. Epithelail cells are active participants in vocal fold wound healing: an in vivo animal model of injury. *PLoS ONE*. 2014;9:e115389.

40. Singer AJ, Clark RA. Cutaneous wound healing. *N Engl J Med*. 1999;341:738-746.

41. Gurtner GC, Werner S, Barrandon Y, Longaker MT. Wound repair and regeneration. *Nature*. 2008;453:314-321.

42. Ling CY, Yamashita M, Waselchuk EA, Raasch J, Bless DM, Welham NV. Alteration in cellular morphology, density and distribution in rat vocal fold mucosa following injury. *Wound Repair Regen*. 2010;18:89-97.

43. Karamichos D, Lakshman N, Petroll WM. An experimental model for assessing fibroblast migration in 3-D collagen matrices. *Cell Motil Cytoskel*. 2009;66:1-9.

44. Xie Y, Rizzi SC, Dawson R, et al. Development of a three-dimensional human skin equivalent wound model for investigating novel wound healing therapies. *Tissue Eng Part C*. 2010;16:1111-1123.

45. Miyazaki K, Oyanagi J, Hoshino D, Togo S, Kumagai H, Miyagi Y. Cancer cell migration on elongate protrusions of fibroblasts in collagen matrix. *Sci Rep*. 2019;9:292.

46. Palencia L, Das A, Pelecek SP, Thibeault SL, Leydon C. Epidermal growth factor mediated healing in stem cell-derived vocal fold mucosa. *J Surg Res*. 2015;197:32-38.

47. Schor SL. Cell proliferation and migration on collagen substrata in vitro. *J Cell Sci*. 1980;41:159-175.

48. Hartman CD, Isenberg BC, Chua SG, Wong JY. Vascular smooth muscle cell durotaxis depends on extracellular matrix composition. *PNAS*. 2016;113:11190-11195.